Modern Management Science & Engineering
ISSN ISSN 2052-2576
Vol. 8, No. 1, 2026
www.scholink.org/ojs/index.php/mmse

Original Paper

Volatile Fatty Acid Production from Chicken Manure under Acidic and Alkaline Anaerobic Fermentation: Ammonia Inhibition and Microbial Mechanisms

Yukang Gu[1*], & Xiao Huang[1]

[1] School of Environmental Science and Engineering, Nanjing University of Information Science & Technology, Nanjing, Jiangsu, China

[*] Corresponding Author

Received: December 28, 2025 Accepted: January 28, 2025 Online Published: February 15, 2026

doi:10.22158/mmse.v8n1p224 URL: http://dx.doi.org/10.22158/mmse.v8n1p224

Abstract

This study investigated the effect of initial pH on volatile fatty acid (VFAs) production during anaerobic fermentation of chicken manure and further elucidated the mechanisms of ammonia inhibition and microbial community dynamics. The results showed that weakly acidic to neutral conditions (pH=5 and 7) were most favorable for VFA accumulation, reaching a maximum of 16264.2 mg COD/L, while strongly acidic (pH=3) or strongly alkaline (pH=11) conditions inhibited VFA production. Under optimal pH conditions, the activation of acidogenic bacteria and the inhibition of methanogens by high ammonia nitrogen concentrations promoted VFA accumulation. Microbial community analysis revealed that Firmicutes and Bacteroidota were the dominant phyla, with Romboutsia and Lactobacillus identified as key genera under acidic conditions, while Bacillus and Bacteroides played crucial roles under neutral conditions. Metagenomic prediction further indicated that carbohydrate and amino acid metabolism were the dominant metabolic pathways, with key functional enzymes including pyruvate ferredoxin oxidoreductase [EC:1.2.7.3], acetyl-CoA carboxylase [EC:6.4.1.2], and phosphoglycerate mutase [EC:5.4.2.12]. This study elucidates the pH-dependent mechanisms of VFA production and identifies the key microbial taxa and enzymatic processes that regulate acidogenic fermentation.

Keywords

resource utilization, fermentation, microbial inhibition, poultry manure valorization

1. Introduction

The rapid expansion of intensive poultry farming has generated substantial quantities of livestock

manure. If not properly managed, this waste poses significant environmental stress, constrains industrial development, even threaten the health of local communities (MA & HUANG, 2024). Anaerobic digestion is a well-established and effective strategy for the resource recovery of poultry manure.

Compared to swine (GüNGöR-DEMIRCI & DEMIRER, 2004) and cattle (MAGBANUA, & ADAMS, 2001) manure, chicken manure (CM) contains substantially higher nitrogen (N) content. This provides a more abundant N source to support protein and enzyme synthesis during fermentation, thereby offering a greater potential for enhanced volatile fatty acid (VFAs) production (QIAO, YAN, YE et al., 2011).

Common strategies to enhance VFAs production from poultry manure include pH regulation, temperature control (WANG, DAI, ZHANG et al., 2018) and adding chemical additives (YUAN, ZHANG, & ZHU, 2021). Among these, pH adjustment is considered particularly promising, as it avoids issues related to carbon source competition (ZHANG, WANG, LI et al., 2018) and secondary contamination (CORRALES-MOYA, BARRANTES, CHACóN-MADRIGAL et al., 2023) from residual additives. The pH is a critical factor directly influencing VFAs yields during fermentation. This is because specific pH conditions selectively enrich or suppress distinct functional microbial populations. Mohanakrishna et al. (2018) reported that neutral to weakly alkaline conditions favored the activity of Lactobacillus, thereby promoting acetate production. Qin et al. (2019) demonstrated that under strongly acidic conditions, *Clostridium* species dominated the acidogenic activity. Subsequent studies[11] have further characterized the competitive dynamics between VFAs-producing genera, particularly the enrichment of *Clostridium* and *Bacillus* under varying pH conditions. However, the functional roles and gene expression profiles of the microbial community driving VFAs synthesis during CM fermentation remain poorly understood.

During anaerobic fermentation, a portion of the produced VFAs is subsequently consumed in the methanogenic phase (NIU, HOJO, QIAO et al., 2014). Therefore, suppressing methanogenesis is essential for achieving VFAs accumulation (CHEN, CHENG, & CREAMER, 2008). High ammonia N concentrations can directly inhibit methanogenic activity (ZHOU, LIU, ZHANG et al., 2023)—a phenomenon known as “ammonia inhibition.” This inhibition occurs because elevated ammonia levels penetrate the methanogen cell membrane, disrupting enzymatic function and energy metabolism. The inhibitory effect of NH_4^+-N on methanogenesis in anaerobic digestion is well documented. Kim et al. (1993) reported significant inhibition at concentrations of 3–5 g/L, while Pakarinen et al. (2008) observed near-complete inhibition at 3–10 g/L. However, for high-N substrates such as CM, the concentration of released ammonia varies with fermentation pH. The resulting effects on VFAs accumulation under these diverse pH conditions remain to be elucidated.

In this study, batch fermentation experiments were conducted with CM as the substrate under various pH conditions to investigate the patterns of VFAs production and accumulation. By integrating the dynamics of inorganic salt release and shifts in microbial community structure during fermentation, this

study elucidates the mechanism by which ammonia nitrogen concentration influences the activity and metabolic function of key microorganisms under different pH conditions. Furthermore, it reveals the biosynthetic pathways and regulatory mechanisms underlying VFA production.

2. Materials and Methods

2.1 The Characteristics of CM

CM was collected from a poultry farm in Nanjing, then dewatered and air-dried. The collected CM was then passed through a stainless steel mesh sieve to remove coarse impurities such as gravel and feathers. The sieved CM was mixed with water, allowed to settle for 24 h, and the supernatant was decanted. The resulting solid was stored at 4 °C until use. The characteristics of the prepared CM are summarized in Table 1.

Table 1. Characteristics of the Chicken Manure

Index	Unit	Data
pH	--	6.40±0.3
ORP	mV	-20.5±10.5
MLVSS	g/L	31±4.8
sCOD	mg/L	7500±300
Protein	mg/L	43±8.5
Carbohydrate	mg/L	130±25
NH_4^+-N	mg/L	300±10
PO_4^{3-}-P	mg/L	350±15

2.2 Fermentation Operation

A 3-L mixture of CM and water was distributed equally into 6 fermentation reactors. The pH in reactors 2–6 was adjusted to 3, 5, 7, 9 and 11, respectively. Using 1 M HCl or NaOH. The pH in reactor 1 was left unadjusted to serve as a control. All reactors were incubated at 35 °C with shaking at 140 rpm for 16 days to ensure uniform dispersion of the reaction mixture. Every 2 days, 20 mL of the CM suspension was withdrawn from each reactor, centrifuged at 10,000 rpm for 10 min, and the supernatant was collected for analysis. The following parameters were measured: pH, ORP, total solids (TS), volatile solids (VS), ammonia nitrogen (NH_4^+-N), orthophosphate (PO_4^{3-}-P), soluble chemical oxygen demand (sCOD), proteins, polysaccharides and VFAs.

2.3 Analysis Methods

2.3.1 Chemical Analysis Methods

Concentrations of sCOD, NH_4^+-N, PO_4^{3-}-P, TS and VS were determined according to standard methods. The pH and ORP were measured directly using a portable digital meter (HQ11D, HACH, USA) after

calibration.Soluble protein was quantified using the bicinchoninic acid (BCA) method with absorbance measured at 562 nm. Polysaccharides were determined by the anthrone-sulfuric acid method, with absorbance read at 620 nm.Volatile fatty acids were analyzed using gas chromatography (Agilent 7890A, USA). Briefly, 1 mL of filtrate was transferred to a GC vial, acidified with 300 μL of formic acid, then injected into the chromatograph. The instrument was equipped with a flame ionization detector (FID). The injector and detector temperatures were both set at 250 °C, with a split ratio of 25:1. The oven temperature was programmed as follows: held at 80 °C for 1 min, then increased to 200 °C at a rate of 10 °C/min. The injection volume was 0.5 μL. N was used as the carrier gas at a flow rate of 25 mL/min. Separation was performed on a DB-FATWAX UI column (30 m × 0.25 mm × 0.25 μm; part No. G3903-63008).

2.3.2 Methods of Microbiological Analysis

To investigate the effect of pH on microbial community characteristics, samples were collected and analyzed. Microbial DNA was extracted from six samples using the PowerSoil DNA Isolation Kit (Mo Bio Laboratories, Carlsbad, CA, USA). Purified DNA was stored at -20 °C prior to analysis. The V3–V4 hypervariable regions of the 16S rRNA gene were amplified by polymerase chain reaction (PCR) using primers 338F (5′-ACTCCTACGGGAGGCAGCA-3′) and 806R (5′-GGACTACCAGGGTATCTAAT-3′). Amplicon sequencing was performed on an Illumina MiSeq platform at Majorbio Bio-Pharm Technology Co., Ltd. (Shanghai, China).

3. Results and Discussion

3.1 Changes of Dissolved Organic Compounds

3.1.1 VFAs

The effect of initial pH on VFAs accumulation during anaerobic fermentation of CM is shown in Fig. 1(A). Under the initial pH=5 condition, the total VFAs accumulation reached 16264.2 mg COD/L, which was slightly higher than those observed at initial pH=7, 9 in the unadjusted control group. In contrast, VFAs accumulation at initial pH=3 was substantially lower than in all other groups, amounting to less than one-fifth of that achieved at pH=5. This finding is consistent with Ma et al. (2024), who reported that extremely low pH markedly suppresses total VFAs production.

The distribution of individual VFAs under different initial pH conditions is presented in Fig. 1 (B). Acetic acid was the dominant VFAs component across all initial pH conditions, its proportion generally increased with increasing pH. Propionic and butyric acids were the next most abundant fractions; both reached their maximum proportions under near-neutral pH and declined as the pH shifted toward either acidic or alkaline extremes. In contrast, the proportions of isobutyric, isovaleric, and valeric acids remained relatively low throughout all treatments. Notably, the highest proportion of acetic acid and the lowest proportion of valeric acid (nearly negligible) were both observed at initial pH=11. These results demonstrate that regulating initial pH significantly influences both the quantity and composition of VFAs during anaerobic fermentation (ZOU, PAN, HE et al., 2018). Alkaline conditions in particular

favor acetic acid accumulation, thereby supporting more efficient resource recovery from CM.

3.1.2 sCOD

The extent of CM hydrolysis during anaerobic fermentation can be evaluated by monitoring sCOD. The effect of initial pH on sCOD during acidogenic fermentation of CM is shown in Fig. 1(C). In all six reactors, the concentrations increased rapidly during the first 4 days of fermentation, peaked at 8 d, then gradually declined before stabilizing. The highest concentration (approximately 12,000 mg/L) was observed at initial pH=5 on 8 d, which was about 1.15 times that of the control group on the same day. With the exception of the pH=3 condition—where sCOD remained below the initial level—sCOD concentrations in all other reactors exceeded that of the raw substrate. This indicates that excessively acidic conditions adversely affect sCOD solubilization. These results demonstrate that adjusting initial pH significantly influences sCOD solubilization from CM, with the highest release observed at pH=5.

3.1.3 Proteins and Polysaccharides

As key constituents of extracellular polymeric substances (EPS), polysaccharides and proteins serve as important indicators of acidogenic fermentation performance. The effect of initial pH on polysaccharide solubilization during anaerobic fermentation of CM is shown in Fig. 1(D).Polysaccharide concentrations fluctuated throughout fermentation. During the initial phase (0–8 d), concentrations increased in the pH=3, 5 and 11 reactors, all peaking at approximately 8 d—with the most pronounced increase observed at pH=11. In the later phase (8–16 d), polysaccharide levels continuously declined, likely due to enhanced microbial metabolic activity that facilitated the conversion of polysaccharides into organic acids.Notably, polysaccharide solubilization varied markedly with initial pH. The highest polysaccharide concentration (1200 mg/L) was observed under strongly alkaline conditions (pH=11), which was significantly higher than that under all other pH conditions. In contrast, under strongly acidic conditions (pH=3), the polysaccharide concentration reached only approximately 50% of that achieved at pH=11. Polysaccharide levels in the other treatment groups (pH=5, 7 and 9) were significantly lower than those in the pH=3 and 11 groups ($p < 0.05$).

The effect of initial pH on protein solubilization during anaerobic fermentation of CM is shown in Fig. 1(E). During the initial phase (0–6 d), protein concentrations increased markedly and peaked at 6 d. The highest concentration (8000 mg/L) was observed at pH=11, which was approximately 1.4 times that of the control group. Thereafter, protein concentrations gradually declined and stabilized after 8 d, ranging from 2000 to 3500 mg/L. During fermentation, proteins are hydrolyzed by proteases into amino acids, which are subsequently deaminated to release free ammonia.

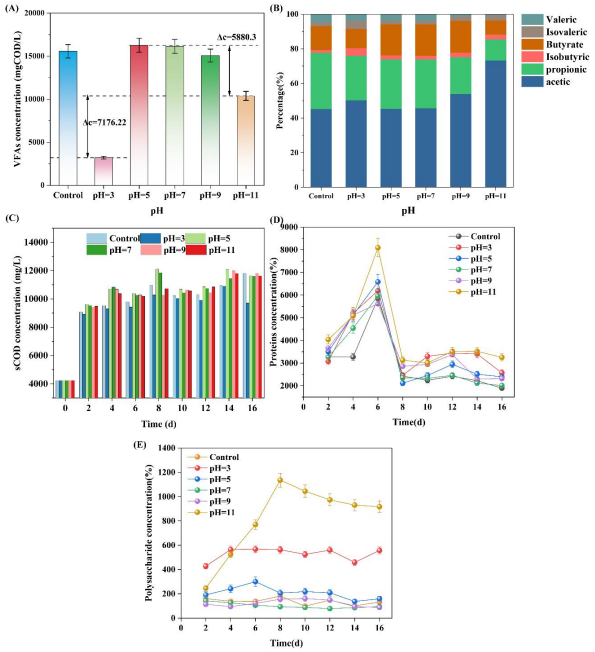

Figure 1. Total VFAs Concentration (A); VFAs Composition (B); sCOD Concentration (C); Protein Concentration (D) and Polysaccharide Concentration (E) during CM Fermentation under Different pH Condition

3.2 pH and ORP

The effect of initial pH on the pH profile during anaerobic fermentation of CM is shown in Fig. 2(A). The pH of the control group remained relatively stable throughout fermentation. Notably, the pH of all other reactors converged toward that of the control at 2 d, then gradually returned to their respective initial values.

The effect of initial pH on oxidation-reduction potential (ORP) during acidogenic fermentation of CM is shown in Fig. 2(B). During the initial phase (0–6 d), ORP fluctuated and then gradually stabilized. As the pH increased from acidic to alkaline, ORP decreased from positive to negative values, with the lowest ORP observed at pH=11. Previous studies[18] have reported that an ORP range of –270 to –290 mV favors anaerobic degradation. Therefore, the alkaline conditions applied in this study, particularly strong alkalinity, were conducive to the anaerobic fermentation of CM.

3.3 Changes of Dissolved Inorganic Salt

The effect of initial pH on NH_4^+-N concentration during acidogenic fermentation of CM is shown in Fig. 2(C). During fermentation, NH_4^+-N concentrations generally followed a pattern of increase, followed by decrease and then another increase. Peak values were observed at approximately 6 d, while the lowest values occurred around 10 d. The release of NH_4^+-N primarily originates from the decomposition of proteins and urea into amino acids (PUASTUTI, YULISTIANI, & HANDIWIRAWAN, 2018), which are further degraded to generate NH_4^+-N. This indicates that amino acid decomposition was most active during the initial (0–6 d) and later (12–16 d) phases of

fermentation. Among all conditions, NH_4^+-N concentrations at pH=3 and 11 were significantly lower than those in the other four groups.

These results demonstrate that initial pH significantly affects NH_4^+-N solubilization from CM. Under neutral to weakly acidic/alkaline conditions (pH=5–9), NH_4^+-N release was enhanced and concentrations were substantially higher. In contrast, strongly acidic (pH=3) and strongly alkaline (pH=11) conditions markedly inhibited NH_4^+-N production. Given that protein concentrations were not suppressed under these extreme pH conditions, it is inferred that such environments likely impair the activity of hydrolytic and acidogenic bacteria (PUASTUTI, YULISTIANI, & HANDIWIRAWAN, 2018), thereby limiting NH_4^+-N generation. Additionally, the oxidative ORP environment observed at pH=3 may have contributed to the low NH_4^+-N concentration through oxidation to nitrate and nitrite (HUANG, ZHANG, ZHAO et al., 2023). The underlying microbial mechanisms require further investigation.

Notably, NH_4^+-N concentration was closely correlated with pH and with VFAs production. Low NH_4^+-N levels (e.g. at pH=3) corresponded to low VFAs yields, while higher NH_4^+-N concentrations under weakly acidic and neutral conditions were associated with substantially higher VFAs accumulation. This positive correlation is consistent with ammonia inhibition: under favorable pH conditions, high NH_4^+-N concentrations are generated during CM fermentation, which suppress methanogenic activity and thereby allow VFAs to accumulate.

The effect of initial pH on PO_4^{3-}-P solubilization during acidogenic fermentation of CM is shown in Fig. 2(D). Overall, the concentrations increased initially and then gradually stabilized. From 0 to 4 d, the concentrations remained low and relatively stable across all six reactors. Between 4 and 6 d, concentrations increased sharply and peaked at 6 d. Thereafter, PO_4^{3-}-P levels gradually stabilized. The concentration decreased as initial pH increased. Under acidic conditions, PO_4^{3-}-P release primarily originated from the decomposition of phospholipids and polyphosphates (NéMETH, CSóKA, SEMNANI JAZANI et al., 2022). Under alkaline conditions, PO_4^{3-}-P was mainly derived from phosphate precipitation. In this study, PO_4^{3-}-P concentrations were substantially higher under acidic conditions than under alkaline conditions. This indicates that acidic environments favor the decomposition of phospholipids and polyphosphates during CM fermentation.

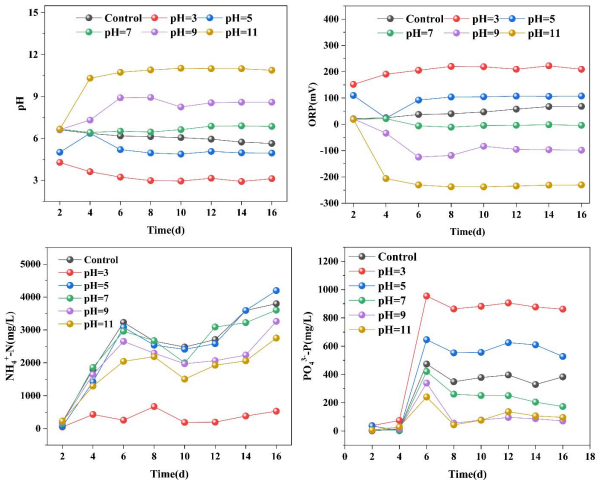

Figure 2. Changes in pH (A); ORP (B); NH_4^+-N Concentration (C) and PO_4^{3-}-P Concentration (D) during Fermentation

3.4 Microbiological Analysis

3.4.1 Diversity and Richness of Microorganisms

The alpha diversity indices of the six experimental samples are presented in Table 2. Microbial richness first decreased and then increased with increasing pH. Higher richness was observed under strongly acidic and strongly alkaline conditions, while lower richness was observed under neutral conditions. A similar trend was observed for the Shannon and Simpson indices: higher Shannon values and lower Simpson values indicate greater microbial community diversity. Among the six experimental groups, the highest microbial richness was observed at pH=9. This finding is consistent with Huang et al.[22], who reported that alkaline conditions can increase bacterial richness. However, richness decreased at pH=11, indicating that excessively strong alkalinity may suppress richness. The highest diversity was observed at pH=3, suggesting that acidic conditions favor microbial community diversity.

Principal component analysis (PCA) was used to identify the principal components in each sample and to visualize the differences and relative distances among samples. As shown in Fig. 3(A), the acidic (pH=3 and 5), neutral (pH=7 and control) and alkaline (pH=9 and 11) groups were distributed in different quadrants. This indicates that distinct pH conditions contributed to microbial community diversity at the OTU level. However, the differences within each pH group were less pronounced, suggesting that the degree of acidity or alkalinity was not the primary driver of this diversity.

Venn diagrams are commonly used to visualize the similarity and diversity of microbial communities. Fig. 3(B) presents the operational taxonomic units (OTUs) detected in each experimental group, revealing substantial variation in OTU composition across groups. The highest number of OTUs was observed at pH=7, while the lowest was found at pH=9. This suggests that weakly alkaline conditions may influence microbial community richness.

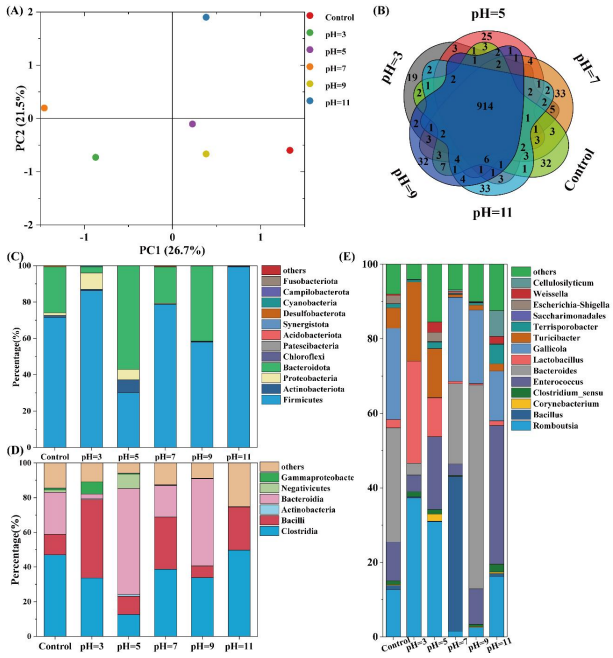

Figure 3. Principal Component Analysis Diagram (A), venn Diagram (B), Microbial Phylum Level Diagram (C), Class Level Diagram (D), Genus Level Diagram (E)

Table 2. Bacterial Richness and Diversity of Samples

Sample	Ace	Chao	Shannon	Simpson
Control	372	391	3.52	0.058
pH=3	480	488	3.63	0.054
pH=5	320	32	2.48	0.172
pH=7	388	325	2.81	0.138
pH=9	563	566	3.05	0.125
pH=11	434	431	3.40	0.087

3.4.2 Microbial Community Composition

The response of the microbial community at the phylum level to different pH conditions is shown in Fig. 3(C). *Firmicutes*, *Bacteroidota* and *Proteobacteria* were the dominant phyla across all conditions, which is consistent with the findings of Slezak et al. (2017). The relative abundance of *Firmicutes* first decreased and then increased with increasing pH. Its abundance reached 86.23% at pH=3 and 99.37% at pH=11, reflecting its strong adaptability to extreme environments. This tolerance is attributed to the ability of *Firmicutes* to form dormant spores with thick cell walls under unfavorable conditions (FILIPPIDOU, JUNIER, WUNDERLIN et al., 2019). In addition, *Firmicutes* comprises various hydrolytic bacteria that can enhance VFAs production, which explains the relatively high concentrations of polysaccharides and proteins observed under strongly alkaline conditions in this study.

Bacteroidota showed higher abundance under neutral conditions, with its relative abundance first increasing and then decreasing as pH increased. The peak abundance was observed at pH=5, while the lowest levels were found at pH=3 and 11. These results indicate that *Bacteroidota* is poorly adapted to strongly acidic or strongly alkaline environments. *Proteobacteria* was more abundant at low pH and decreased sharply under neutral and alkaline conditions, suggesting a positive correlation with acidic environments and inhibition under alkaline conditions. Previous studies have reported that most *Proteobacteria* are involved in hydrolysis and acidification (ATASOY, EYICE, SCHNüRER et al., 2019). This suggests that *Proteobacteria* contributed substantially to hydrolytic acidification at low pH in this study.

The response of the microbial community at the class level to different pH conditions is shown in Fig. 3(D). Among the major classes identified, *Bacteroidia*, *Bacilli* and *Clostridia* were the dominant taxa. *Bacilli* and *Clostridia* exhibited high relative abundance under both strongly acidic and strongly alkaline conditions, indicating their tolerance to extreme pH environments. This finding is consistent with the results reported by Ma et al. (2024). *Bacteroidia* showed the highest abundance under weakly acidic, weakly alkaline and neutral conditions, while its abundance was suppressed under strongly acidic and strongly alkaline conditions. This trend is consistent with the observations described above. Notably, the relative abundance of *Gammaproteobacteria* was higher under low pH conditions (pH=3–7) than in other groups. As a member of the phylum *Proteobacteria*, this class is known for its strong capacity to degrade organic matter, particularly under heterogeneous environmental conditions (LIU, LI, MA et al., 2019). This suggests that the pH=5 reactor possessed a high potential for organic matter degradation.

The response of the microbial community at the genus level to different pH conditions is shown in Fig. 3(E). The dominant genera varied considerably with pH. Under acidic conditions, *Romboutsia*, *Lactobacillus* and *Turicibacter* were the predominant taxa, with *Romboutsia* accounting for 38.53% of the relative abundance. However, the abundances of these genera decreased sharply as pH increased, a trend consistent with the findings of Huang et al.[27]. Under neutral and weakly alkaline conditions, *Bacillus*, *Bacteroides* and *Enterococcus* were the dominant genera. Notably, *Bacillus* accounted for 42.68% of the relative abundance at pH=7 but was nearly undetectable in all other groups. This indicates that Bacillus has a narrow pH tolerance and is strongly inhibited under both acidic and alkaline conditions. Under strongly alkaline conditions, *Enterococcus* exhibited the highest relative abundance, reaching 37.56%.

3.5 Correlations between Microorganisms and Environmental Factors

The correlations among microbial genera in the CM fermentation broth are shown in Fig. 4(A) using Pearson's correlation coefficient. As the dominant genera under acidic conditions, *Romboutsia*, *Clostridium_sensu_stricto_1* and *Turicibacter* were positively correlated with one another, a pattern also observed by Wang et al. (2014). The first two genera are commonly found in intestinal microbiota and were primarily responsible for the decomposition of proteins and polysaccharides in this study. In

addition, *Clostridium_sensu_stricto_1* and *Turicibacter* have been reported to play a positive role in fermentation under acidic conditions (YANG, ZHUO, ZHONG et al., 2023). In contrast, the dominant genera under alkaline conditions, including *Bacteroides*, *Enterococcus* and *Bacillus*, showed limited correlation with one another. Bacillus in particular exhibited a negative correlation with most other genera.

The correlation heatmap between microbial genera and soluble substrates is shown in Fig. 4(B), which identifies the genera most closely associated with each substrate. *Gallicola*, *Bacteroides*, *Corynebacterium* and *Bacillus* showed strong correlations with VFAs production. These genera contributed most to acidogenesis, and most of them were also dominant under neutral and weakly alkaline conditions, where VFAs yields were the highest. *Enterococcus* was positively correlated only with acetic acid among all VFAs. Previous studies have reported that this genus is involved in hydrogen production, accompanied by rapid acetate generation (YIN & WANG, 2019). In contrast, the dominant genera under acidic conditions, including *Romboutsia*, *Clostridium_sensu_stricto_1* and *Turicibacter*, exhibited strong negative correlations with VFAs yields and individual VFAs. Although these genera have been reported to participate in carbohydrate metabolism under anaerobic conditions (GERRITSEN, HORNUNG, RENCKENS et al., 2017), it is inferred that they contributed to polysaccharide hydrolysis but were inhibited in amino acid fermentation under acidic pH. Notably, these genera were also strongly correlated with PO_4^{3-}-P and ORP. At pH=3, the ORP remained at approximately 200 mV, indicating a strongly acidic and oxidative environment (GRIMALT-ALEMANY, ETLER, ASIMAKOPOULOS et al., 2021). Under such conditions, organic phosphorus compounds in the fermentation broth were directly hydrolyzed, some polyphosphate-accumulating organisms (PAOs) underwent cell lysis (WU, PENG, WANG et al., 2010), resulting in elevated PO_4^{3-}-P concentrations.

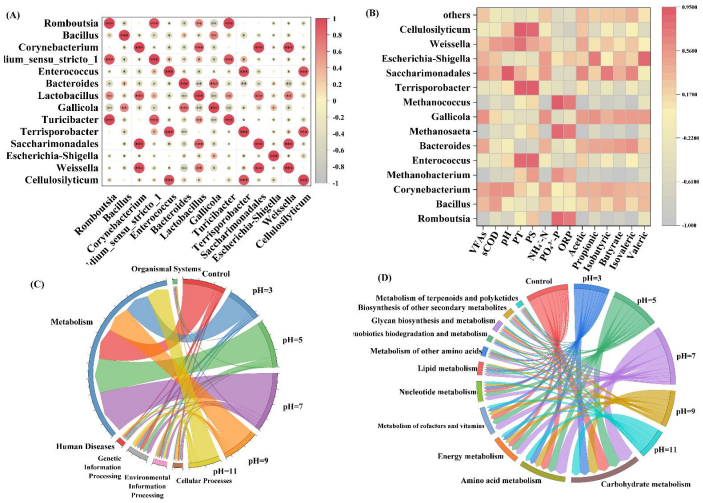

Figure 4. Correlation of Microorganisms within groups (A), Correlation of Microbial Genera with Key Indicators (B), Functional Classification (level 1) (C), Metabolic Pathways (level 2) (D)

3.6 Microbial Function Prediction and Metabolic Pathways

PICRUSt is a bioinformatics tool that infers metagenomic functional profiles based on 16S rRNA gene sequencing data and reference databases (DOUGLAS, BEIKO, & LANGILLE, 2018). The functional profiles of the microbial communities under different pH conditions are shown in Fig. 4(C). Metabolism was the predominant functional category across all groups, accounting for 73%–78% of the total abundance. This indicates that VFAs production during CM fermentation was primarily driven by metabolic processes, followed by genetic information processing and other categories. This finding is consistent with the results reported by Luo et al. (2022). The relative abundance of metabolism-related functions showed no substantial variation among groups, although slightly higher proportions were observed at pH=5 and 7, suggesting that microbial metabolic activity was enhanced under neutral and weakly acidic conditions. The predominant metabolic pathways are presented in Fig. 4(D). Carbohydrate metabolism accounted for the highest proportion (23%–28%), followed by amino acid metabolism (15%–17%) and energy metabolism (14%–16%). These three pathways, which play dominant roles in VFAs production, also exhibited their highest relative abundances under neutral and weakly acidic conditions. This suggests that weakly acidic environments can substantially stimulate carbohydrate metabolism (LUO, WANG, CHENG et al., 2021).

Further analysis was conducted on functional abundances at KEGG Level 3. Within carbohydrate metabolism (Fig. 5(A)), the most abundant pathways were ko00620 (pyruvate metabolism), ko00520 (amino sugar and nucleotide sugar metabolism) and ko00010 (glycolysis). Their relative abundances generally increased with increasing pH, peaked at approximately pH=7, then declined. The abundant pathways within amino acid metabolism are shown in Fig. 5(B). ko00270 (cysteine and methionine metabolism) was the predominant pathway and is involved in the Stickland reaction (LI, HE, YAN et al.). Other abundant pathways included ko00260 and ko00250, all of which also peaked at approximately pH=7. The abundant pathways within energy metabolism are presented in Fig. 5(C). ko00190 (oxidative phosphorylation) and ko00720 (carbon fixation pathways in prokaryotes) exhibited the highest abundances, indicating that these pathways contributed most to energy supply during microbial fermentation. Notably, all three metabolic categories exhibited their highest relative abundances under neutral and weakly acidic conditions. This indicates that extreme pH conditions (pH=3 and 11) inhibit microbial fermentation metabolism in CM, whereas weakly acidic or neutral conditions (pH=5 and 7) are conducive to metabolic activity. This promotional effect was more pronounced for amino acid metabolism and energy metabolism.

FAPROTAX (Functional Annotation of Prokaryotic Taxa) is a database used to analyze the abundance of bacterial or archaeal taxa and to predict metagenomic functional profiles. The functional distribution of microbial communities predicted by FAPROTAX is shown in Fig. 5(D). Most functional categories exhibited relative abundances below 5% across all experimental groups, with the exception of chemoheterotrophy and fermentation, both of which showed high abundances in the pH=3 group. This indicates that chemoheterotrophic and fermentative activities were highly active under strongly acidic

conditions. Chemoheterotrophic microorganisms, which utilize organic compounds as carbon sources, energy sources and electron donors, include various decomposing bacteria that play key roles in the degradation of amino acids and proteins (LIU, SUN, ZHAO et al., 2021). This also explains why the NH_4^+-N concentration at pH=3 was significantly lower than that in other groups. Although fermentation-related functions were highly abundant at pH=3, VFAs production remained low. This is attributed to a higher proportion of gas-producing fermentation over acidogenic fermentation, leading to the generation of gases such as CO_2 rather than VFAs. Previous studies have reported that Lactobacillus can produce gas during fermentation (HERTZBERGER, PRIDMORE, GYSLER et al., 2013), a phenomenon that was more pronounced under strongly acidic conditions in this study.

The functional profiles predicted by Bugbase are shown in Fig. 5(E). Among these functions, Anaerobic and Potentially Pathogenic exhibited high relative abundances. This is attributed to the predominantly anaerobic fermentation environment and the fact that the CM feedstock was collected from a poultry farm, where the presence of pathogens is more likely. Notably, Gram Positive showed high functional abundance under strongly alkaline conditions. This is consistent with the dominance of Gram-positive bacteria in this environment. However, the abundances of *Clostridium* and *Bacillus*, which are known to participate in anaerobic organic decomposition, were relatively low. The predominant Gram-positive genus was Enterococcus, which has been reported to serve as an indicator bacterium for fecal antibiotic resistance (FATOBA, ABIA, AMOAKO et al., 2021).

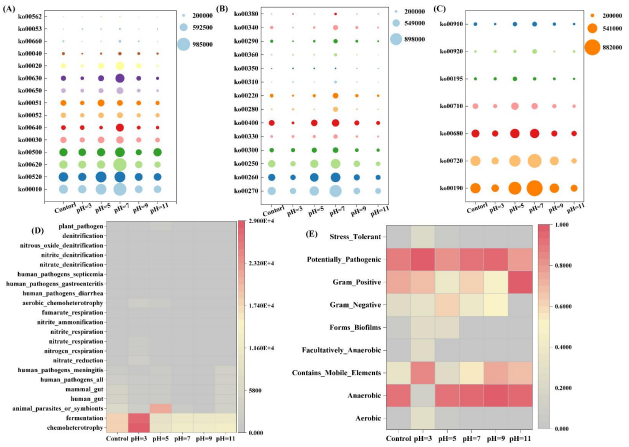

Figure 5. Carbohydrate Metabolism (A); Amino Acid Metabolism (B); Energy Metabolism (C); Functional Prediction Using Farprotax (D) and Functional Prediction Using BugBase (E)

3.7 Metabolic Pathways and Enzyme Analysis

3.7.1 TCA Cycle

The tricarboxylic acid (TCA) cycle represents a central catabolic pathway for carbohydrates, lipids and proteins. The most abundant enzymes were pyruvate ferredoxin oxidoreductase [EC:1.2.7.3] and 2-oxoglutarate ferredoxin oxidoreductase [EC:1.2.7.11], both of which are involved in the conversion of 2-oxoglutarate to succinyl-CoA (Fig. 6(A)). Pyruvate ferredoxin oxidoreductase [EC:1.2.7.3]

catalyzes the oxidative decarboxylation of pyruvate to acetyl-CoA, a metabolite closely associated with acetate production (FURDUI & RAGSDALE, 2000; ZHOU, LAMA, JIANG et al., 2020). In this study, the activities of these enzymes peaked at pH=5 and were substantially upregulated under both pH=5 and 7 conditions. This indicates that weakly acidic and neutral environments significantly enhanced enzyme activities.

3.7.2 3-HP Cycle

The 3-hydroxypropionate (3-HP) cycle is a carbon fixation pathway that uses acetyl-CoA and CO_2 as substrates to synthesize organic carbon compounds while regenerating acetyl-CoA (ALCAMáN-ARIAS, PEDRóS-ALIó, TAMAMES et al., 2018). In this cycle, acetyl-CoA is carboxylated to malonyl-CoA by acetyl-CoA carboxylase [EC:6.4.1.2]. The intermediates propionyl-CoA and succinyl-CoA can be converted to methylmalonyl-CoA via propionyl-CoA carboxylase [EC:6.4.1.3] and methylmalonyl-CoA epimerase [EC:5.1.99.1], respectively, which can re-enter the TCA cycle and ultimately regenerate acetyl-CoA. This process indirectly influences acetate synthesis and has been proposed as a key determinant of VFAs production (TAMAKI, NISHINO, OGAWA et al., 2019). As shown in Fig. 6(B), the activities of key enzymes in this cycle, including acetyl-CoA carboxylase [EC:6.4.1.2] and succinyl-CoA synthetase [EC:6.2.1.3], peaked at pH=5 and 7. This suggests that weakly acidic and neutral conditions favor the initiation of the 3-HP cycle, with acetyl-CoA serving as the starting substrate (HüGLER, HUBER, STETTER et al., 2003).

3.7.3 Glycolysis

Glycolysis serves as a core driver of acidogenic fermentatio and its optimization can substantially enhance short-chain fatty acid production. Pyruvate, the end product of glycolysis, not only acts as a precursor for acidogenesis but also fuels the 3-HP cycle after conversion to acetyl-CoA. Carbohydrates are first hydrolyzed to glucose, which is then converted to fructose by glucose-6-phosphate isomerase [EC:5.3.1.9]. Subsequent enzymatic reactions sequentially produce glyceraldehyde-3-phosphate, glycerate and phosphoenolpyruvate, ultimately yielding pyruvate. The abundant enzymes identified in this study, including phosphoglycerate mutase [EC:5.4.2.12] and another enzyme with the same EC number, are primarily involved in the conversion of glyceraldehyde-3-phosphate to glycerate and both peaked under weakly acidic and neutral conditions (Fig. 6(C)). Elevated abundance of enzymes catalyzing the G3P-to-glycerate conversion has been reported to indicate active glycolytic acidogenesis (SIROVER, 2011), which regulates the downstream production of pyruvate and VFAs.

The three metabolic pathways described above are closely interconnected through the central hubs pyruvate and acetyl-CoA. Changes in pH modulate enzyme activities, thereby affecting the production of these two intermediates and ultimately influencing VFAs yields. In all cases, enzyme activities were highest under weakly acidic and neutral conditions (pH=5 and 7).

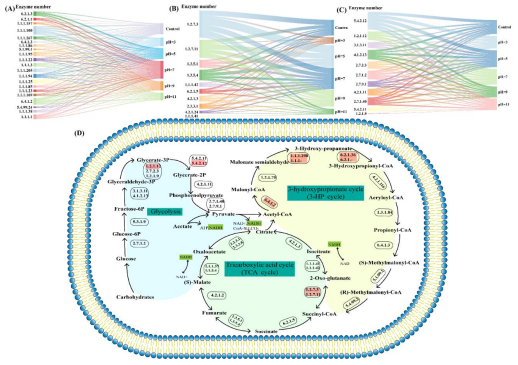

Figure 6. Relative Abundance of Key Enzymes in 3-HP cycle (A); Relative Abundance of Key Enzymes in Glycolysis (B); Relative Abundance of Key Enzymes in TCA Cycle (C) and Diagrams of Key Enzymes Pathway (D)

4. Conclusion

Initial pH significantly affected VFAs accumulation during CM fermentation. The highest VFAs accumulation was observed under weakly acidic to neutral conditions (pH=5 and 7). In contrast, strongly acidic (pH=3) or strongly alkaline (pH=11) environments suppressed VFAs production, although the proportion of acetic acid remained relatively high. Mechanistic analysis revealed that the positive effect of weakly acidic to neutral pH on acidogenesis was achieved through two primary pathways. First, it enhanced the activity of key acidogenic genera, thereby increasing VFAs production. Second, it elevated NH_4^+-N concentrations, which inhibited methanogens and allowed VFAs to accumulate. In addition, key functions and enzyme activities involved in acidogenic pathways were substantially upregulated at pH=5 and 7.

References

MA, S., & HUANG, X. (2024). Volatile fatty acid (VFA) production from sludge and chicken manure co-fermentation: Role of acid/alkali-treatment and microbial characteristics. *Journal of Environmental Chemical Engineering*, *12*(2), 112215.

GüNGöR-DEMIRCI, G., & DEMIRER, G. N. (2004). Effect of initial COD concentration, nutrient addition, temperature and microbial acclimation on anaerobic treatability of broiler and cattle manure. *Bioresource technology*, *93*(2), 109-17.

MAGBANUA, J. R. B. S., ADAMS, T. T., & JOHNSTON, P. (2001). Anaerobic codigestion of hog and poultry waste. *Bioresource technology*, *76*(2), 165-8.

QIAO, W., YAN, X., YE, J. et al. (2011). Evaluation of biogas production from different biomass wastes with/without hydrothermal pretreatment. *Renewable energy*, *36*(12), 3313-8.

WANG, G., DAI, X., ZHANG, D. et al. (2018). Two-phase high solid anaerobic digestion with dewatered sludge: Improved volatile solid degradation and specific methane generation by temperature and pH regulation. *Bioresource technology*, *259*(253), 8.

YUAN, H., ZHANG, D., & ZHU, N. (2021). Exogenous pH Buffer System with K 2 HPO 4/KH 2 PO 4 Addition Improving Thermophilic High-Solid Anaerobic Digestion of Waste-Activated Sludge. *Journal of Environmental Engineering*, *147*(2), 04020155.

ZHANG, T., WANG, B., LI, X. et al. (2018). Achieving partial nitrification in a continuous post-denitrification reactor treating low C/N sewage. *Chemical Engineering Journal*, *335*(330), 7.

CORRALES-MOYA, J., BARRANTES, G., CHACóN-MADRIGAL, E. et al. (2023). A potential consequence for urban birds' fitness: Exposed anthropogenic nest materials reduce nest survival in the clay-colored thrush. *Environmental Pollution*, *326*(121456).

MOHANAKRISHNA, G., ABU-REESH, I. M., AL-RAOUSH, R. I. et al. (2018). Cylindrical graphite based microbial fuel cell for the treatment of industrial wastewaters and bioenergy generation. *Bioresource technology*, *247*(753), 8.

QIN, L., & GAO, X. (2019). Recycling of waste autoclaved aerated concrete powder in Portland cement by accelerated carbonation. *Waste Management*, *89*(254), 64.

WU, L., YANG, Y., GUO, W. et al. (2020). Deterioration of biological pollutants removal induced by linear alkylbenzene sulphonates in sequencing batch reactors: Insight of sludge characteristics, microbial community and metabolic activity. *Bioresource Technology*, *315*(123843).

NIU, Q., HOJO, T., QIAO, W. et al. (2014). Characterization of methanogenesis, acidogenesis and hydrolysis in thermophilic methane fermentation of chicken manure. *Chemical Engineering Journal*, *244*(587), 96.

CHEN, Y., CHENG, J. J., & CREAMER, K. S. (2008). Inhibition of anaerobic digestion process: A review. *Bioresource technology*, *99*(10), 4044-4064.

ZHOU, X., LIU, T., ZHANG, S. et al. (2023). Metagenomic insight of fluorene-boosted sludge acidogenic fermentation: Metabolic transformation of amino acids and monosaccharides. *Science of The Total Environment*, *865*(161122).

KIM, I. H., CHO, M. H., & WANG, S. S. (1993). Measurement of hydrodynamic shear by using a dissolved oxygen probe. Biotechnology and bioengineering, *41*(3), 296-302.

ZOU, J., PAN, J., HE, H. et al. Nitrifying aerobic granular sludge fermentation for releases of carbon source and phosphorus: The role of fermentation pH. *Bioresource Technology*, *260*(30), *7*.

MAHESH, G. B., & MANU, B. (2019). Biological treatment of 3, 6-dichloro-2-methoxybenzoic acid using anaerobic-aerobic sequential batch reactor. *Environmental Processes*, *6*(493-509).

PUASTUTI, W., YULISTIANI, D., & HANDIWIRAWAN, E. (2018). Supplementation of molasses and branched-chain amino acid to increase in vitro digestibility of ammoniated corn cob in ruminants feed. *Jurnal Ilmu Ternak dan Veteriner*, *22*(4), 179-187.

HUANG, S., ZHANG, B., ZHAO, Z. et al. (2023). Metagenomic analysis reveals the responses of microbial communities and nitrogen metabolic pathways to polystyrene micro (nano) plastics in activated sludge systems. *Water Research*, *241*(120161).

NéMETH, Z., CSóKA, I., SEMNANI, JAZANI, R. et al. (2022). Quality by design-driven zeta potential optimisation study of liposomes with charge imparting membrane additives. *Pharmaceutics*, *14*(9), 1798.

HUANG, H., LIU, H., ZHANG, R. et al. (2022). Effect of slow-released biomass alkaline amendments oyster shell on microecology in acidic heavy metal contaminated paddy soils. *Journal of Environmental Management*, *319*(115683).

SLEZAK, R., GRZELAK, J., KRZYSTEK, L. et al. (2017). The effect of initial organic load of the kitchen waste on the production of VFA and H2 in dark fermentation. *Waste Management*, *68*(610-7.

FILIPPIDOU, S., JUNIER, T., WUNDERLIN, T. et al. (2019). Adaptive strategies in a poly-extreme environment: Differentiation of vegetative cells in Serratia ureilytica and resistance to extreme conditions. *Frontiers in microbiology*, *10*(102).

ATASOY, M., EYICE, O., SCHNüRER, A. et al. (2019). Volatile fatty acids production via mixed culture fermentation: Revealing the link between pH, inoculum type and bacterial composition. *Bioresource Technology*, *292*(121889).

LIU, G., LI, X., MA, X. et al. (2019). Hydrolysis and decomposition of waste activated sludge with combined lysozyme and rhamnolipid treatment: Effect of pH. *Bioresource Technology*, *293*(122074).

HUANG, X., & XIANG, Z. (2024). Enhanced volatile fatty acids production in thermal hydrolysis pretreatment with constant pH regulation: Effects evaluation and mechanism elucidation. *Journal of Environmental Chemical Engineering*, *12*(6), 114830.

WANG, H., ZHANG, Z,, LI, F. et al. (2024). The effects of dietary fermented soybean residue on the growth, antioxidant capacity, digestive enzyme activities, and microbial compositions of the intestine in Furong crucian carp (Furong carp♀× Red crucian carp♂). *Fishes*, *9*(4), 138.

YANG, W., ZHUO, Q., ZHONG, Y. et al. (2023). Effects of Iron Nanoparticles Addition on Bacterial Community and Phytotoxicity in Aerobic Compost of Pig Manure. *Agronomy*, *13*(5), 1239.

YIN, Y., & WANG, J. (2019). Optimization of fermentative hydrogen production by Enterococcus faecium INET2 using response surface methodology. *International Journal of Hydrogen Energy*, *44*(3), 1483-1491.

GERRITSEN, J., HORNUNG, B., RENCKENS, B. et al. (2017). Genomic and functional analysis of Romboutsia ilealis CRIBT reveals adaptation to the small intestine. *Peer J*, *5*(e3698).

GRIMALT-ALEMANY, A., ETLER, C., ASIMAKOPOULOS, K. et al. (2021). ORP control for boosting ethanol productivity in gas fermentation systems and dynamics of redox cofactor NADH/NAD+ under oxidative stress. *Journal of CO2 Utilization*, *50*(101589).

WU, C., PENG, Y., WANG, S. et al. (2010). Effect of enhancing denitrifying phosphorus removal on microbial population variation in A2O process. *J Chem Ind Eng (CHN)*, *61*(186-191).

DOUGLAS, G. M., BEIKO, R. G., & LANGILLE, M. G. (2018). Predicting the functional potential of the microbiome from marker genes using PICRUSt. *Microbiome analysis: Methods and protocols*, 169-177.

LUO, J., LI, Y., LI, H. et al. (2022). Deciphering the key operational factors and microbial features associated with volatile fatty acids production during paper wastes and sewage sludge co-fermentation. *Bioresource Technology*, *344*(126318).

LUO, J., WANG, F., CHENG, X. et al. (2021). Metatranscriptomic insights of the metabolic process enhancement during food wastes fermentation driven by linear alkylbenzene sulphonates. *Journal of Cleaner Production*, *315*(128145).

LI, N., HE, J., YAN, H. et al. (2017). Pathways in bacterial and archaeal communities dictated by ammonium stress in a high solid anaerobic digester with dewatered sludge. *Bioresource Technology*, *241*(95-102).

LIU, L., SUN, F,, ZHAO, H. et al. (2021). Compositional changes of sedimentary microbes in the Yangtze River Estuary and their roles in the biochemical cycle. *Science of The Total Environment*, *760*(143383).

HERTZBERGER, R. Y., PRIDMORE, R. D., GYSLER, C. et al. (2013). Oxygen relieves the CO2 and acetate dependency of Lactobacillus johnsonii NCC 533. *PLoS One*, *8*(2), e57235.

FATOBA, D. O., ABIA, A. L. K., AMOAKO, D. G. et al. (2021). Rethinking manure application: Increase in multidrug-resistant enterococcus spp. In agricultural soil following chicken litter application. *Microorganisms*, *9*(5), 885.

FURDUI, C., & RAGSDALE, S. W. (2000). The role of pyruvate ferredoxin oxidoreductase in pyruvate synthesis during autotrophic growth by the Wood-Ljungdahl pathway. *Journal of Biological Chemistry*, *275*(37), 28494-9.

ZHOU, S., LAMA, S., JIANG, J. et al. (2020). Use of acetate for the production of 3-hydroxypropionic acid by metabolically-engineered Pseudomonas denitrificans. *Bioresource Technology*, *307*(123194).

ALCAMáN-ARIAS, M. E., PEDRóS-ALIó, C., TAMAMES, J. et al. (2018). Diurnal changes in active carbon and nitrogen pathways along the temperature gradient in Porcelana hot spring microbial mat. *Frontiers in microbiology*, *9*(2353).

TAMAKI, S., NISHINO, K., OGAWA, T. et al. (2019). Comparative proteomic analysis of mitochondria isolated from Euglena gracilis under aerobic and hypoxic conditions. *Plos one*, *14*(12), e0227226.

HüGLER, M., HUBER, H., STETTER, K. O. et al. (2003). Autotrophic CO 2 fixation pathways in archaea (Crenarchaeota). *Archives of microbiology*, *179*(160-73.

SIROVER, M. A. (2011). On the functional diversity of glyceraldehyde-3-phosphate dehydrogenase: biochemical mechanisms and regulatory control. *Biochimica et Biophysica Acta (BBA)-General Subjects*, *1810*(8), 741-51.